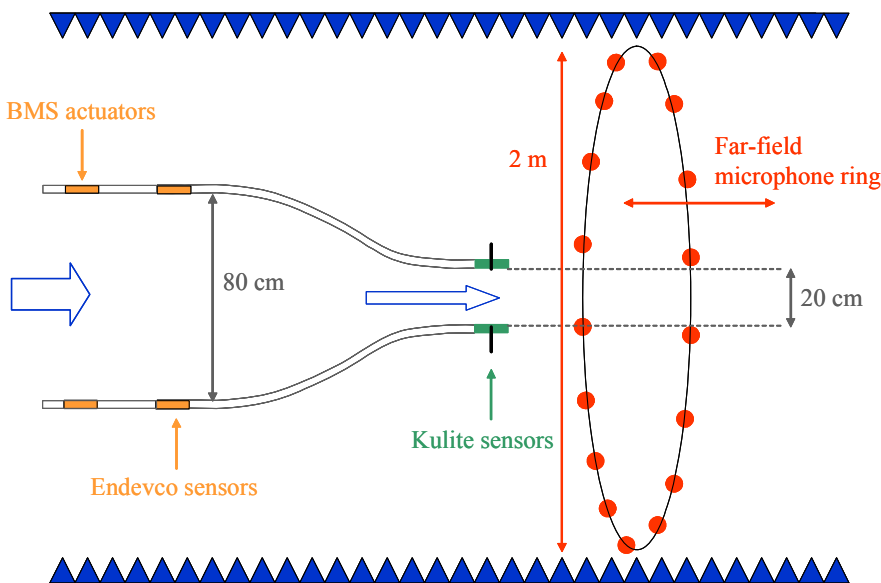




## Executive summary

# In-Duct and Far-Field Mode Detection Techniques for Engine Exhaust Noise Measurements

AIAA Paper 2007-3439



### Problem area

Aft radiating turbo-machinery noise is one of the major noise components of current aircraft engines. To investigate noise reduction concepts, computational methods for noise radiation through an engine exhaust are being developed, amongst others at NLR. One of the objectives of the EU-funded research project TURNEX is the experimental validation of such computational prediction methods for turbo-machinery noise radiation through the engine exhaust. For that purpose, in November 2006 experimental data

were acquired in the QinetiQ anechoic test facility NTF on scaled exhaust models with realistic flow conditions in the duct and in the exhaust jet. To generate in-duct noise sources for these validation tests, EADS-IW developed a mode synthesizer featuring 30 actuators and 30 sensors, which is able to generate azimuthal modes in the range of  $m = -14$  to  $m = +14$ . Thus, well-defined sound fields can be generated for numerical code validation, and also for parametric studies.

Validation of the prediction methods is done by measuring the

### Report no.

NLR-TP-2007-347

### Author(s)

P. Sijtsma  
J. Zillmann

### Report classification

UNCLASSIFIED

### Date

May 2007

### Knowledge area(s)

Aeroacoustic & Experimental  
Aerodynamics

### Descriptor(s)

Mode detection  
Microphone arrays  
Ducted flow  
Free jets  
Far field

in-duct modal structure at a location downstream of the mode-synthesizer, and also in the far field. The in-duct measurements serve as input for the prediction methods, and the far-field data are used for validation. Although the mode synthesizer is able to generate single modes, it is still necessary to measure modes, because scattering of modes is likely to occur due to deviations of the axisymmetry. Prior to the main experimental program at QinetiQ, in September 2005 a pre-test with this mode synthesizer was conducted in the NLR Small Anechoic Wind Tunnel KAT. This pre-test was carried out to test the mode synthesizer, to investigate measurement techniques for mode detection in the presence of high speed flow, and to identify solutions to any problems that may arise. These tests were carried out using a convergent wind tunnel nozzle of circular cross-section with diameter varying from 80 cm in the upstream part to 20 cm in the downstream part. At the nozzle exhaust a free jet was generated at Mach numbers up to 0.7. In the upstream wide part of the nozzle, tonal acoustic modes were generated by the mode synthesizer of EADS-IW. Inside the nozzle, near the exhaust, azimuthal mode spectra were determined with a circular array of 64 flush-mounted transducers. In the far-field, around the free jet, mode spectra were measured with a 2 m diameter

traversable circular array of 92 microphones.

### **Description of work**

This paper treats 4 different techniques for azimuthal mode detection by circular microphone arrays inside a flow duct, and in the far field around a free jet. The following techniques for mode detection are considered:

- Conventional RMS-averaging.
- Diagonal Removal (DR)
- Cross-correlation with a reference channel (CC)
- Principal Component analysis (PC)

The mode detection techniques were applied to the experimental data of the KAT experiment. In-duct and far-field applications were considered separately because of the different background noise properties.

### **Results and conclusions**

It is argued that the best mode detection results are obtained with the CC method and the PC method. Furthermore, the mode measurements showed the ability of the mode synthesizer to generate prescribed modes, which was one of the main objectives of the tests.

### **Applicability**

The conclusions of this paper are applied to the post-processing of the data from the large scale rig experiment in the QinetiQ-NTF facility.



NLR-TP-2007-347

## In-Duct and Far-Field Mode Detection Techniques for Engine Exhaust Noise Measurements

AIAA Paper 2007-3439

P. Sijtsma and J. Zillmann<sup>1</sup>

<sup>1</sup> EADS Innovation Works

This report is based on a presentation held on the 13th AIAA/CEAS Aeroacoustics Conference, Rome, 21-23 May, 2007.

The contents of this report may be cited on condition that full credit is given to NLR and the authors.

This publication has been refereed by the Advisory Committee AEROSPACE VEHICLES.

Customer	European Union
Contract number	516079
Owner	National Aerospace Laboratory NLR
Division	Aerospace Vehicles
Distribution	Unlimited
Classification of title	Unclassified
	July 2008

Approved by:

Author	Reviewer	Managing department
 11/8/08	 11/8/08.	 10/10

## Summary

This paper treats 4 different techniques for azimuthal mode detection by circular microphone arrays inside a flow duct, and in the far field around a free jet. In-duct and far-field applications are considered separately because of the different background noise properties. The mode detection techniques were applied to experimental data from tests in the NLR small anechoic wind tunnel facility KAT. These tests were carried out using a convergent wind tunnel nozzle of circular cross-section with diameter varying from 80 cm in the upstream part to 20 cm in the downstream part. At the nozzle exhaust a free jet was generated at Mach numbers up to 0.7. In the upstream wide part of the nozzle acoustic modes were generated by the mode synthesizer of EADS-IW. Tonal sound was generated by a circular phased array of 30 actuators, which provided azimuthal modes in the range of  $m = -14$  to  $m = +14$ . Inside the nozzle, near the exhaust, azimuthal mode spectra were determined with a circular array of 64 flush-mounted transducers. In the far-field, around the jet, mode spectra were measured with a 2 m diameter traversable circular array of 92 microphones. It is argued that the best mode detection results are obtained with a technique based on cross-correlation with a reference signal, or with a technique based on principal component analysis. The mode measurements showed the ability of the mode synthesizer to generate prescribed modes, which was one of the main objectives of the tests

## **Contents**

<b>In-Duct and Far-Field Mode Detection Techniques</b>	<b>4</b>
<b>Nomenclature</b>	<b>4</b>
<b>I. Introduction</b>	<b>5</b>
<b>II. Experimental set-up</b>	<b>5</b>
<b>III. Processing techniques</b>	<b>7</b>
<b>IV. Applications</b>	<b>10</b>
<b>V. Appraisal of mode synthesizer</b>	<b>15</b>
<b>VI. Conclusion</b>	<b>16</b>
<b>Acknowledgments</b>	<b>16</b>
<b>References</b>	<b>16</b>

# In-Duct and Far-Field Mode Detection Techniques

Pieter Sijtsma\*

*National Aerospace Laboratory NLR, 8300 AD Emmeloord, The Netherlands*

and

Jörgen Zillmann†

*EADS Innovation Works Germany, 81663 Munich, Germany*

This paper treats 4 different techniques for azimuthal mode detection by circular microphone arrays inside a flow duct, and in the far field around a free jet. In-duct and far-field applications are considered separately because of the different background noise properties. The mode detection techniques were applied to experimental data from tests in the NLR small anechoic wind tunnel facility KAT. These tests were carried out using a convergent wind tunnel nozzle of circular cross-section with diameter varying from 80 cm in the upstream part to 20 cm in the downstream part. At the nozzle exhaust a free jet was generated at Mach numbers up to 0.7. In the upstream wide part of the nozzle acoustic modes were generated by the mode synthesizer of EADS-IW. Tonal sound was generated by a circular phased array of 30 actuators, which provided azimuthal modes in the range of  $m = -14$  to  $m = +14$ . Inside the nozzle, near the exhaust, azimuthal mode spectra were determined with a circular array of 64 flush-mounted transducers. In the far-field, around the jet, mode spectra were measured with a 2 m diameter traversable circular array of 92 microphones. It is argued that the best mode detection results are obtained with a technique based on cross-correlation with a reference signal, or with a technique based on principal component analysis. The mode measurements showed the ability of the mode synthesizer to generate prescribed modes, which was one of the main objectives of the tests.

## Nomenclature

CC	= mode detection technique based on Cross-Correlation with reference signal
DR	= mode detection technique based on Diagonal Removal
PC	= mode detection technique based on Principal Component analysis
RMS	= mode detection technique based on Root Mean Squares
SNR	= Signal to Noise Ratio
SP	= Signal Prominence (difference between first and second eigenvalue)
TvA	= Target versus Actual (difference between target mode and prevailing other mode)
$A_m$	= mode power
$\hat{A}_m$	= estimated mode power
$a_m$	= mode amplitude
<b>C</b>	= cross-power matrix
$C_{kl,j}$	= cross-spectrum
$E_m$	= mode power due to background noise
$\mathbf{e}_v$	= eigenvector of cross-power matrix
$f$	= frequency
$G$	= array gain

---

\* Senior Scientist, Department of Helicopters & Aeroacoustics, P.O. Box 153.

† Scientist, Department of Structures Engineering, Production & Mechatronics.



$i$	=	imaginary unit
$j$	=	frequency index
$K$	=	number of microphones
$k, l$	=	microphone indices
$M$	=	Mach number of jet flow
$m$	=	azimuthal mode number
$N$	=	number of averages
$p_k(f)$	=	complex pressure amplitude
$Q$	=	noise power
$S$	=	block size: number of samples used as input for FFT
$s$	=	sample index
$t$	=	time
$\varepsilon_k$	=	random noise
$\phi_k$	=	angular position of microphone $k$
$\chi_k(t)$	=	pressure fluctuation in microphone $k$
$\chi_{k,s}$	=	sampled pressure fluctuation in microphone $k$
$\Delta t$	=	time interval between two samples
$\lambda_v$	=	eigenvalue of cross-power matrix
$v$	=	eigenvalue index
$\theta$	=	polar angle of far-field array

## I. Introduction

ONE of the objectives of the EU-funded research project TURNEX is the experimental validation of computational prediction methods for turbo-machinery noise radiation through the engine exhaust. For that purpose, in November 2006 experimental data were acquired in the QinetiQ anechoic test facility NTF on scaled exhaust models with realistic flow conditions in the duct and in the exhaust jet. To generate in-duct noise sources for these validation tests, EADS-IW developed a mode synthesizer featuring 30 actuators and 30 sensors, which is able to generate azimuthal modes in the range of  $m = -14$  to  $m = +14$ . Thus, well-defined sound fields can be generated for numerical code validation, and also for parametric studies.

Validation of the prediction methods is done by measuring the in-duct modal structure at a location downstream of the mode-synthesizer, and also in the far field. The in-duct measurements serve as input for the prediction methods, and the far-field data are used for validation. Although the mode synthesizer is able to generate single modes, it is still necessary to measure modes, because scattering of modes is likely to occur due to deviations of the axisymmetry.

Prior to the main experimental program at QinetiQ, in September 2005 a pre-test with this mode synthesizer was conducted in the NLR Small Anechoic Wind Tunnel KAT. This pre-test was carried out to test the mode synthesizer, to investigate measurement techniques for mode detection in the presence of high speed flow, and to identify solutions to any problems that may arise, in particular coherence losses caused by the jet shear layer. Mode measurements were done with an in-duct and a far-field microphone array.

This paper discusses techniques to determine azimuthal mode breakdowns of tonal sound using measured data from both the in-duct and the far-field array. In-duct mode detection may be a well-established technique<sup>1,2</sup>, but it is nevertheless worthwhile to perform investigations on the detection techniques, as the mode detection is done in a high speed flow with high background noise levels. Mode detection in the far field has been applied less often<sup>3</sup>.

In Section II of this paper the experimental set-up is briefly described. Then, in Section III a review is given of 4 different mode detection techniques. In Section IV these techniques are applied to the measured data, and judged on their merits. Finally, in Section V the appraisal of the mode synthesizer is discussed.

## II. Experimental set-up

The set-up of the pre-test in the NLR anechoic facility KAT featured a convergent wind tunnel nozzle with circular cross-section (see Fig. 1). The nozzle diameter varied from 80 cm down to 20 cm. In the wide part of the nozzle azimuthal acoustic modes were generated by the mode synthesizer of EADS-IW. In the narrow part the transmitted acoustic modes were measured with an equidistant circular array of 64 Kulite transducers, mounted flush in the duct wall. The acoustic modes radiating to the far field were measured with a large-size traversable array of 92 microphones, mounted on a 2 m diameter ring (Fig. 2). The jet flow characteristics were measured at a

number of radial and axial positions. The maximum flow Mach number in the 20 cm diameter free jet was  $M = 0.7$ .

The mode synthesizer generated acoustic modes using 30 BMS-4540ND compression drivers, mounted flush in the wall of the wide part (80 cm) of the nozzle. The actuators were mounted as an equidistant circular array at fixed axial position. By this actuator array, azimuthal modes in the range of  $m = -14$  to  $m = +14$  could be generated. Each mode  $m$  is accompanied by alias modes  $m \pm 30k$ , but in the narrow part of the duct these higher order modes were cut-off in most cases. Controlling of the modes was done with a circular array of 30 Endevco transducers, 40 cm downstream of the actuators. At this Endevco array the nozzle diameter was still 80 cm.

The mode detection array near the exhaust consisted of 64 Kulite sensors, spaced equidistantly. Thus, azimuthal modes could be detected in the range of  $m = -31$  to  $m = +31$ . The far-field microphone array consisted of 92 LinearX-M51 microphones, and was therefore able to detect modes between  $m = -45$  and  $m = +45$ . Measurements were performed under the following parameter conditions:

- Far-field array positions (polar angles):  $\theta = 30^\circ, 45^\circ, \dots, 120^\circ$
- Flow speed:  $M = 0.0, 0.5, 0.6, 0.7$
- Frequencies:  $f = 2800, 5600, \dots, 16800$  Hz
- Azimuthal modes:  $m = -14$  to  $m = +14$

Obviously, it was not feasible to perform a full test matrix with all possible combinations ( $7 \times 4 \times 6 \times 29 = 4872$ ) of the parameters described above. Therefore, a test program was put together on the basis of a number of questions:

- Can we recognize far-field modes and directivity?
- Do we have coherence loss for increasing frequency?
- Is coherence loss dependent on Mach number?
- Is coherence loss dependent on mode number?
- Is coherence loss dependent on array position?

Thus, 85 data points at several parameter combinations were acquired.

The questions about coherence loss (due to sound transmission through the jet shear layer) could be answered quickly, since coherence loss and the associated phenomenon of spectral broadening (“haystacking”) were not observed. At any case where the SNR (Signal to Noise Ratio) was sufficiently high the speaker tone appeared as a single peak in the far-field microphone spectra. For frequencies up to 11200 Hz there appeared to be no shear layer induced coherence loss. At higher frequencies we could not observe coherence loss because the SNR was too low.

Nevertheless, the 85 data points contained enough information to test several mode detection techniques, and to make an appraisal of the mode synthesizer.

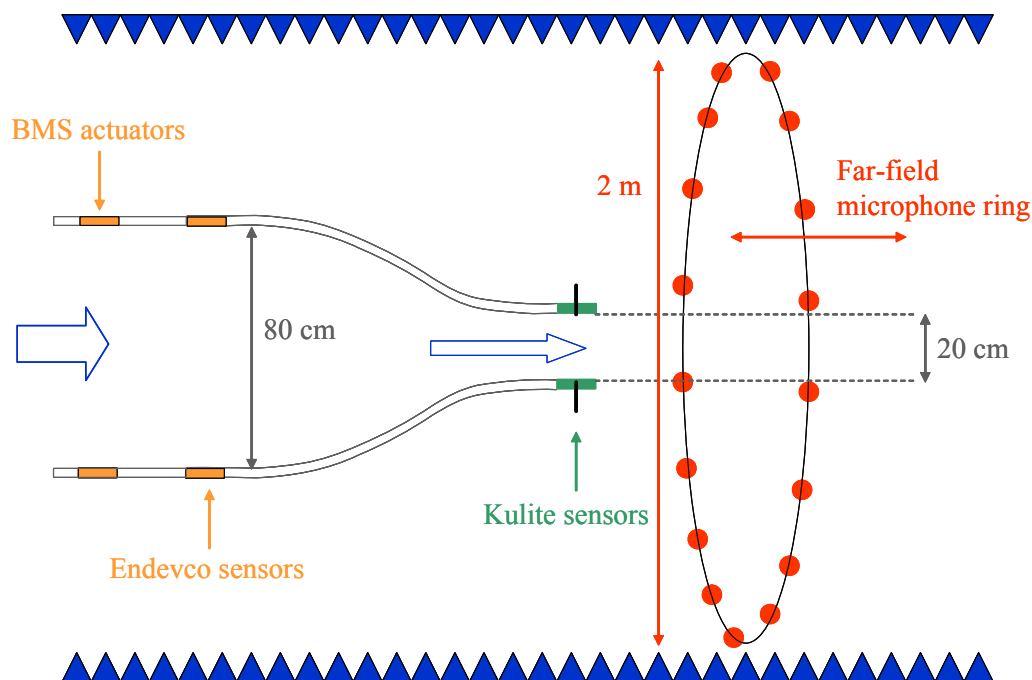


Figure 1. Schematic overview of test set-up in NLR-KAT.



Figure 2. Test set-up; view towards collector (nozzle is covered with acoustic foam).

### III. Processing techniques

#### A. Frequency spectra

Suppose that the pressure fluctuations  $\chi_k(t)$  in microphone  $k$  are sampled as

$$\chi_{k,s} = \chi_k(s\Delta t). \quad (1)$$

Complex pressure amplitudes  $p_k(f)$  of microphone signals are obtained by evaluating a discrete Fourier transform for a block of  $S$  samples:

$$p_k(f) = \frac{2}{S} \sum_{s=1}^S \chi_{k,s} e^{-2\pi i f s \Delta t}. \quad (2)$$

Powers of 2 are used for the block size  $S$ , so that a Fast Fourier Transform (FFT) can be applied to evaluate Eq. (2) at once for the entire relevant range of frequencies, which is

$$f_j = \frac{j}{S\Delta t}, \quad j = 1, \dots, S/2 - 1. \quad (3)$$

Thus, we obtain complex pressure amplitudes:

$$p_{k,j} = p_k\left(\frac{j}{S\Delta t}\right) = \frac{2}{S} \sum_{s=1}^S \chi_{k,s} e^{-2\pi i j s / S}. \quad (4)$$

Note that the Fourier transforms of Eq. (4) are performed without using a “window.” Throughout this report no windows are used. Cross-spectra  $C_{kl,j}$ ,  $j = 1, \dots, S/2 - 1$  are defined by

$$C_{kl,j} = \frac{1}{2} \langle p_{k,j} p_{l,j}^* \rangle, \quad (5)$$

where the asterisk stands for complex conjugation and the brackets mean “averaged over a number of FFT blocks.”

**A**

### B Mode detection

The following techniques for mode detection are considered:

- Conventional rms-averaging (RMS)
- Diagonal Removal (DR)
- Cross-correlation with a reference channel (CC)
- Principal Component analysis (PC)

Mode detection is done at fixed frequencies. Therefore, we will not use the frequency index  $j$  in the following. The mode detection techniques start from a simple delay-and-sum algorithm. Let  $\phi_k$  be the angular position of microphone  $k$ , and  $K$  the number of microphones, then the complex mode amplitude  $a_m$  can be evaluated as

$$a_m = \frac{1}{K} \sum_{k=1}^K p_k e^{im\phi_k}, \quad (6)$$

Herein, the complex pressure amplitude  $p_k$  is obtained by a single FFT block, as in Eq. (4).

### C Conventional rms-averaging (RMS)

Averaging over several FFT blocks can be done by taking the mean squared absolute value of  $a_m$ . This leads to the following expression for the mode power  $A_m$ :

$$A_m = \frac{1}{2} \langle |a_m|^2 \rangle = \frac{1}{2K^2} \left\langle \sum_{k=1}^K \sum_{l=1}^K p_k e^{im\phi_k} p_l^* e^{-im\phi_l} \right\rangle = \frac{1}{K^2} \sum_{k=1}^K \sum_{l=1}^K e^{im\phi_k} \frac{1}{2} \langle p_k p_l^* \rangle e^{-im\phi_l} = \frac{1}{K^2} \sum_{k=1}^K \sum_{l=1}^K e^{im\phi_k} C_{kl} e^{-im\phi_l}. \quad (7)$$

This technique is called the RMS method.

When the microphone signals  $p_k$  are distorted by random noise  $\varepsilon_k$ , then the estimated mode powers  $\tilde{A}_m$  will deviate from the actual values  $A_m$ . In fact, the background noise induces a mode spectrum by itself:

$$E_m = \frac{1}{K^2} \sum_{k=1}^K \sum_{l=1}^K e^{im\phi_k} \frac{1}{2} \langle \varepsilon_k \varepsilon_l^* \rangle e^{-im\phi_l}. \quad (8)$$

After averaging over a large number of FFT blocks, we have

$$\tilde{A}_m = \frac{1}{K^2} \sum_{k=1}^K \sum_{l=1}^K e^{im\phi_k} \frac{1}{2} \langle (p_k + \varepsilon_k)(p_l + \varepsilon_l)^* \rangle e^{-im\phi_l} = A_m + E_m. \quad (9)$$

At the in-duct array, where the (boundary layer) noise is incoherent from one microphone to the other, Eq. (8) simplifies to

$$E_m = \frac{1}{K^2} \sum_{k=1}^K \frac{1}{2} \langle |\varepsilon_k|^2 \rangle. \quad (10)$$

If the noise level is independent of microphone, say  $\frac{1}{2} \langle |\varepsilon_k|^2 \rangle = Q$ , then Eq. (10) further reduces to

$$E_m = \frac{Q}{K}. \quad (11)$$

Thus, it can be derived that the array gain (expected difference between SNR at individual microphones and SNR of calculated mode power) of this array algorithm, as applied to the in-duct measurements, is

$$G_{\text{in-duct}} = 10 \times \log(K) . \quad (12)$$

In the far-field, where the background noise is not incoherent, the array gain is less. If the background noise would be completely incoherent, we would have

$$G_{\text{far-field}} = 10 \times \log(\sqrt{K}) . \quad (13)$$

#### D Diagonal Removal (DR)

The fact that boundary layer noise is incoherent from microphone to microphone can be exploited by removing the main diagonal of the cross-power matrix in Eq. (7), so that the following estimate remains:

$$\tilde{A}_m = \frac{1}{K(K-1)} \sum_{k=1}^K \sum_{\substack{l=1 \\ l \neq k}}^K e^{im\phi_k} C_{kl} e^{-im\phi_l} . \quad (14)$$

Likewise, the background noise mode spectrum will be

$$E_m = \frac{1}{K(K-1)} \sum_{k=1}^K \sum_{\substack{l=1 \\ l \neq k}}^K e^{im\phi_k} \frac{1}{2} \langle \varepsilon_k \varepsilon_l^* \rangle e^{-im\phi_l} . \quad (15)$$

For incoherent (in-duct) background noise, expression (15) vanishes by averaging. In that case, we can derive the following expression for the array gain:

$$G_{\text{in-duct}} = 10 \times \log(K\sqrt{N}) , \quad (16)$$

where  $N$  is the number of averages. Hence, by averaging, the influence of noise can be eliminated. In the far field, however, Eqs. (9) and (13) still apply.

A disadvantage of the DR method is that Eq. (14) can lead to negative answers, which is not physical for a mean-squares expression. Suppose, for example, that the cross-power matrix  $\mathbf{C}$  is induced by a single mode  $n$  with unit strength, and that the number of microphones is  $K = 64$ . In that case we find  $A_n = 1$ , as it should. However, for  $m \neq n$  we find  $A_m = -1/(K-1)$ , instead of zero. These negative ‘‘side lobes’’ may strongly influence secondary genuine modes. If a secondary mode exists with a level 15 dB below the main mode, then the side lobes of the main mode will affect this secondary mode such that its level calculated by Eq. (14) is 18 dB (instead of 15 dB) below the main mode.

#### E Cross-correlation with reference channel (CC)

An other alternative for Eq. (7) is obtained by considering cross-correlations with a reference channel  $k = 0$ , for example a microphone close to the actuators. Then we have, instead of Eq. (6),

$$a_m = \frac{1}{K} \sum_{k=1}^K p_k p_0^* e^{im\phi_k} / (p_0 p_0^*)^{1/2} , \quad (17)$$

This expression is then directly averaged, instead of the squared absolute values:

$$\langle a_m \rangle = \frac{1}{K} \sum_{k=1}^K e^{im\phi_k} \langle p_k p_0^* / (p_0 p_0^*)^{1/2} \rangle . \quad (18)$$

Assuming that the denominator in Eq. (18) is constant (independent of FFT block), we can derive

$$\tilde{A}_m = \frac{1}{2} |\langle a_m \rangle|^2 = \frac{1}{K^2 C_{00}} \left| \sum_{k=1}^K e^{im\phi_k} C_{k0} \right|^2 \approx A_m + \frac{1}{N} E_m. \quad (19)$$

This means that the noise contribution vanishes by averaging, also in the far field. For the array gain we have

$$\begin{cases} G_{\text{in-duct}} = 10 \times \log(KN), \\ G_{\text{far-field}} = 10 \times \log(\sqrt{KN}). \end{cases} \quad (20)$$

Comparing Eqs. (12), (13), (16) and (20) with each other, it seems to be that the CC method is the best that we have considered so far. The CC method does not yield negative answers, like the PC method. The CC method relies on coherence between the reference channel and the azimuthal mode to be measured. In the far field there is a risk that some coherence is lost due to the propagation through the shear layer. Inside the duct the best mode detection technique seems to be the CC method anyway.

## F Principal Component analysis (PC)

A different approach to the elimination of noise is the use of eigenvalue analysis. Since the cross-power matrix is hermitian and positive definite, it can be decomposed as

$$\mathbf{C} = \sum_{\nu=1}^K \lambda_{\nu} \mathbf{e}_{\nu} \mathbf{e}_{\nu}^*, \quad (21)$$

where  $\lambda_{\nu}$  are the (real and nonnegative) eigenvalues, and  $\mathbf{e}_{\nu}$  the normalized eigenvectors (which form an orthogonal set). The asterisk now stands for complex conjugate transposition. If the signal level is sufficiently large compared to the noise (the SNR may be below 0 dB), then the signal is for the most part concentrated in the first principal component. This is the component of Eq. (21) with the highest eigenvalue (say  $\lambda_1$ ). The noise is contained in the other components.

Using these properties, we can define the PC method, which starts from the same double summation, Eq. (7), as the RMS method. However, only the signal part ( $\nu=1$ ) of  $\mathbf{C}$  is included now, and the noise part ( $\nu>1$ ) is eliminated. This leads to

$$A_m = \frac{1}{K^2} \sum_{k=1}^K \sum_{l=1}^K e^{im\phi_k} \lambda_1 (\mathbf{e}_1 \mathbf{e}_1^*)_{kl} e^{-im\phi_l} = \frac{\lambda_1}{K^2} \left| \sum_{k=1}^K e^{im\phi_k} e_{1,k} \right|^2. \quad (22)$$

In the far field the PC method may be a good alternative for the CC method, because it does not suffer from loss of coherence between the reference channel and the array signals. There only needs to be mutual coherence between the signals of the array microphones.

A disadvantage of this technique is that it doesn't perform well when there is too much background noise. Then, the first principal component may contain noise, or may even be dominated by noise. Averaging over more FFT blocks will not remedy this.

To check the quality of the results we will use the "Signal Prominence" (SP), which is defined as the ratio between the first and the second eigenvalue. It is postulated that an SP-level of approximately 6 dB is sufficiently high to assume that the first principal component is dominated by the (tonal) signal. For background noise, the difference between the principal components is usually less.

## IV. Applications

In this section mode spectra are discussed that were obtained from the measured in-duct and far-field array data, using the 4 different techniques of Section III. For the CC method we used as reference the signal of one of the Endeveco sensors in the wide part of the nozzle (Fig. 1). It might have been better to use a signal by which the speakers were driven, but these signals were not recorded. As stated in Section III, the PC method is expected to give accurate results if the SP-levels are sufficiently high. By comparing with the PC method, we can thus also check the accuracy of the other methods.

### A. In-duct modes

A typical result is given in Fig. 3, which shows the in-duct mode spectrum at  $f = 14000$  Hz and  $M = 0.6$  (target mode  $m = 3$ ), calculated by the 4 mode detection techniques. It is observed that the results of the PC method and the CC method are close to each other. The RMS method suffers apparently from too much background noise. The DR method seems to give values that are too low.

The averaged noise floor of the RMS method is 88.9 dB. This is 17.8 dB below the background noise level, which is 106.7 dB. This corresponds with the predicted gain of Eq. (12), which amounts to 18.1 dB ( $K = 64$ ). For the DR method and the CC method the array gain follows from Eqs. (16) and (20). Since the number of averages was  $N = 500$ , these gain levels are 31.6 dB and 45.1 dB, respectively.

For the example shown in Fig. 3 the SP-level is 2.97 dB. Even for this quite low value the PC method and the CC method yield almost the same mode levels, especially at the dominant modes. Except for one data point, the in-duct SP-levels of all other data points are much higher, ranging from 5.9 dB up to 27.8 dB with flow, and 45.3 dB without flow. For all these data points the results of the PC method and the CC method are very close to each other, especially at the dominant modes. The data point with the least agreement is shown in Fig. 4 ( $M = 0.7$ ,  $f = 7200$  Hz,  $m = 11$ ). Here the SP-level is 5.9 dB. A very good example is shown in Fig. 5 ( $M = 0.6$ ,  $f = 5600$  Hz,  $m = 10$ ), for which the SP-level is 27.8 dB. For this case, the results of the PC method and the CC method are practically identical.

At one data point ( $M = 0.6$ ,  $f = 16800$  Hz,  $m = 3$ ) the SP-level is 1.3 dB, which seems to be too low for the PC method. The results are shown in Fig. 6. Even for this case, the difference in peak level between the PC method and the CC method is less than 1 dB.

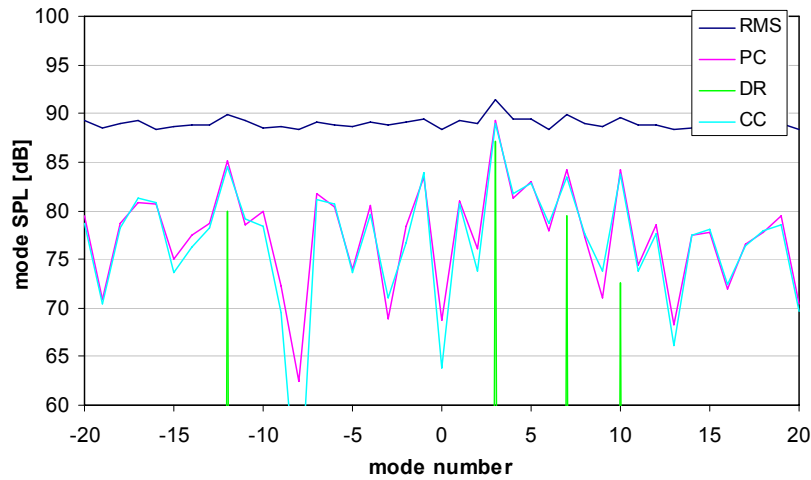


Figure 3. In-duct mode spectrum calculated by 4 different techniques,  $M = 0.6$ ,  $f = 14000$  Hz, target  $m = 3$ .

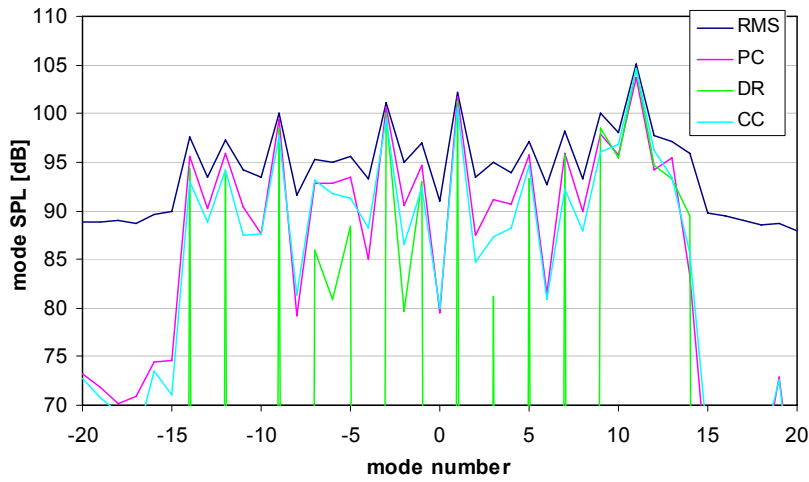


Figure 4. In-duct mode spectrum calculated by 4 different techniques,  $M = 0.7$ ,  $f = 7200$  Hz, target  $m = 11$ .

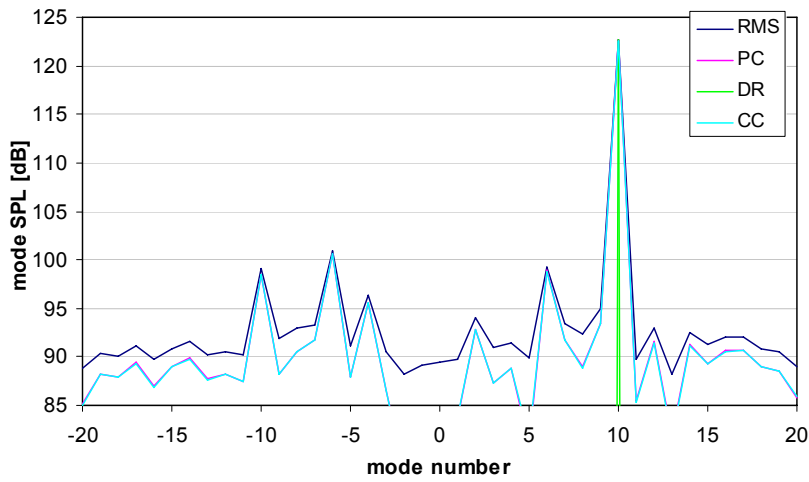


Figure 5. In-duct mode spectrum calculated by 4 different techniques,  $M = 0.6$ ,  $f = 5600$  Hz, target  $m = 10$ .

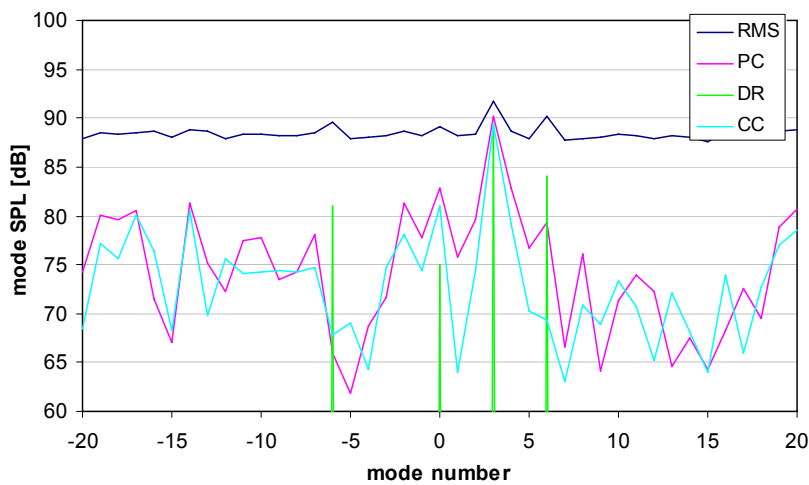


Figure 6. In-duct mode spectrum calculated by 4 different techniques,  $M = 0.6$ ,  $f = 16800$  Hz, target  $m = 3$ .

## B. Far-field modes

In the far-field, the array gain of the CC-method is less than in the duct (see Eq. (20)). Furthermore, the CC method, which assumes coherence with a reference signal, can be affected by coherence loss through the shear layer. Therefore, the CC method might not be as good as for the in-duct array, and it may be better to rely on the PC method.

In the far-field 4 data points had SP-levels below 2 dB, which is too low for a reliable determination of mode levels using the PC method. For these data points (which had nonzero jet flow) the far-field polar angles ( $\theta$ ) were small. The radiation into small angles is usually low in the case of jet flow (cf. “zone of silence” in a shear flow<sup>4</sup>). As an example of such a data point (SP = 0.9 dB), Fig. 7 shows results at  $M = 0.6$ ,  $f = 2800$  Hz,  $\theta = 30^\circ$ , and target  $m = 3$ . Note that only for the CC method the dominant mode is the same as the target mode. Apparently, the first principal component at  $f = 2800$  Hz contains background noise instead of tonal sound produced by the actuators.

All the other data points have SP-levels above 5 dB. The highest SP-level that was found with flow was 26.3 dB, and 41.4 dB without flow. Most of these data points show only little difference in mode levels between the PC method and the CC method. Only for one data point ( $M = 0.6$ ,  $f = 8400$  Hz,  $\theta = 30^\circ$ , target  $m = 5$ ), where SP = 6.0 dB, some more difference is found (see Fig. 8). This may be related to the very low SNR in this case (-9.4 dB)\*. When the SNR is not that low, e.g., for the data point with  $M = 0.7$ ,  $f = 2800$  Hz,  $\theta = 60^\circ$ , and  $m = 3$ , where SP = 5.6 dB and SNR = -4.7 dB, the results are good (see Fig. 9). Very good agreement between the PC method and the CC method is shown in Fig. 10 ( $M = 0.6$ ,  $f = 5600$  Hz,  $\theta = 105^\circ$ ,  $m = 10$ ), for which the SP-level is 19.9 dB. The results of Fig. 10 are from the same data point as Fig. 5.

Note that the results in Figs. 7 to 9 show that the DR method does not give significant improvement compared with the RMS method. This is in agreement with Section III.A.D, where it was stated that Eq. (13) for the far-field array gain holds for both the RMS method and the DR method.

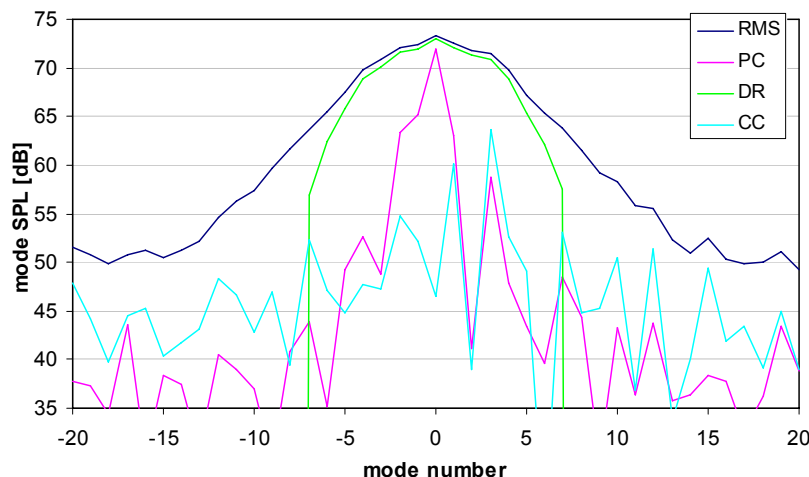


Figure 7. Far-field mode spectrum calculated by 4 different techniques,  $M = 0.6$ ,  $f = 2800$  Hz,  $\theta = 30^\circ$ , target  $m = 3$ .

\* The SNR is defined here as the difference in level between the first eigenvalue and the levels measured with background noise measurements.

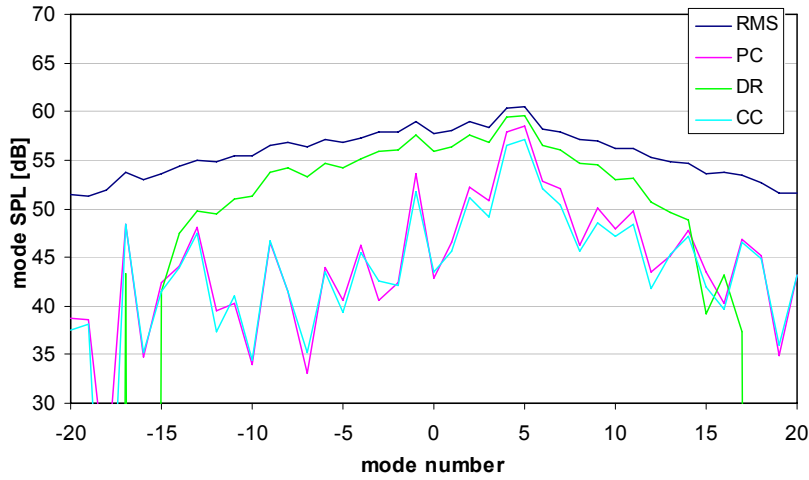


Figure 8. Far-field mode spectrum calculated by 4 different techniques,  $M = 0.6$ ,  $f = 8400$  Hz,  $\theta = 30^\circ$ , target  $m = 5$ .

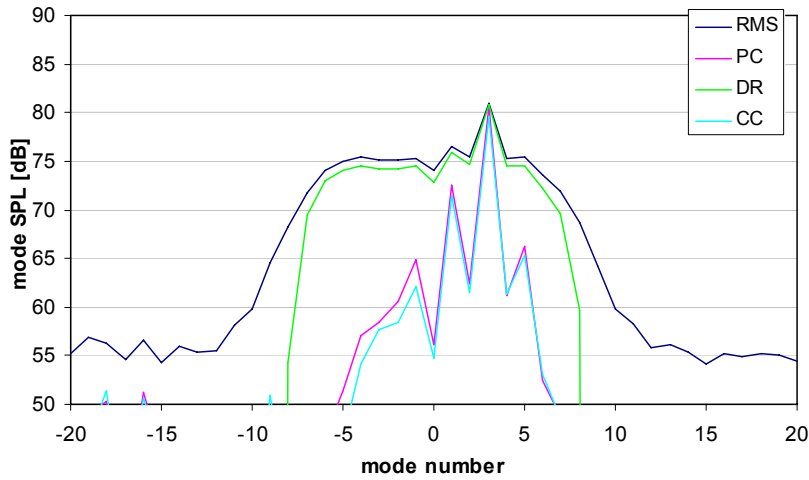


Figure 9. Far-field mode spectrum calculated by 4 different techniques,  $M = 0.7$ ,  $f = 2800$  Hz,  $\theta = 60^\circ$ , target  $m = 3$ .

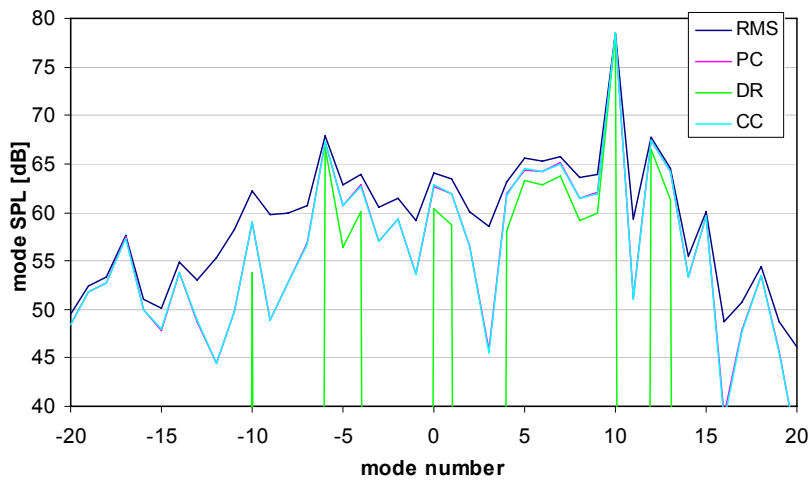


Figure 10. Far-field mode spectrum calculated by 4 different techniques,  $M = 0.6$ ,  $f = 5600$  Hz,  $\theta = 105^\circ$ , target  $m = 10$ .

## V. Appraisal of mode synthesizer

To assess the validity of the mode synthesizer to generate prescribed modes, “Target versus Actual” (TvA)-levels were introduced as the difference between the level of the target mode and the highest level of the remaining modes (see Fig. 11). So, whenever this value (in dB) is positive, the target mode is dominant. The TvA-levels were calculated for all data points, both for the in-duct and for the far-field array. Use has been made of the PC method to calculate the mode levels.

In general, the TvA-levels of the in-duct array were higher than those of the far-field array. Furthermore, there was a tendency towards lower TvA-levels when the frequency increased. Also there was a tendency towards lower TvA-levels with increasing mode number.

For the in-duct array the TvA-levels varied from  $-9.8$  dB to  $22.1$  dB. Only for three data points negative TvA-levels were found. The target modes of these were close to cut-off. For the far-field array the TvA-levels varied from  $-22.8$  dB to  $20.1$  dB. There were 23 data points with negative TvA-levels, and 62 with positive TvA-levels in the far field.

There may be a number of reasons why the far-field TvA-levels are, in general, lower than the in-duct counterparts. One of the possible reasons is the far-field directivity, which may be such that the level of the target mode is relatively low at the measured polar angle. Other reasons may be (small deviations) in the axisymmetric geometry, and loss of coherence. Surprisingly, there is also a number of data points for which the TvA-level in the far field was higher than in the duct. Also this may be attributed to different far-field directivity of different modes.

Since many data points show high TvA-levels (above 5 dB), it can be concluded that the mode synthesizer performed well. In Fig. 12 mode spectra are shown of an example of a “good” data point (the same as Figs. 5 and 10). Here the TvA-level is  $22.1$  dB in the duct, and  $11.0$  dB in the far-field.

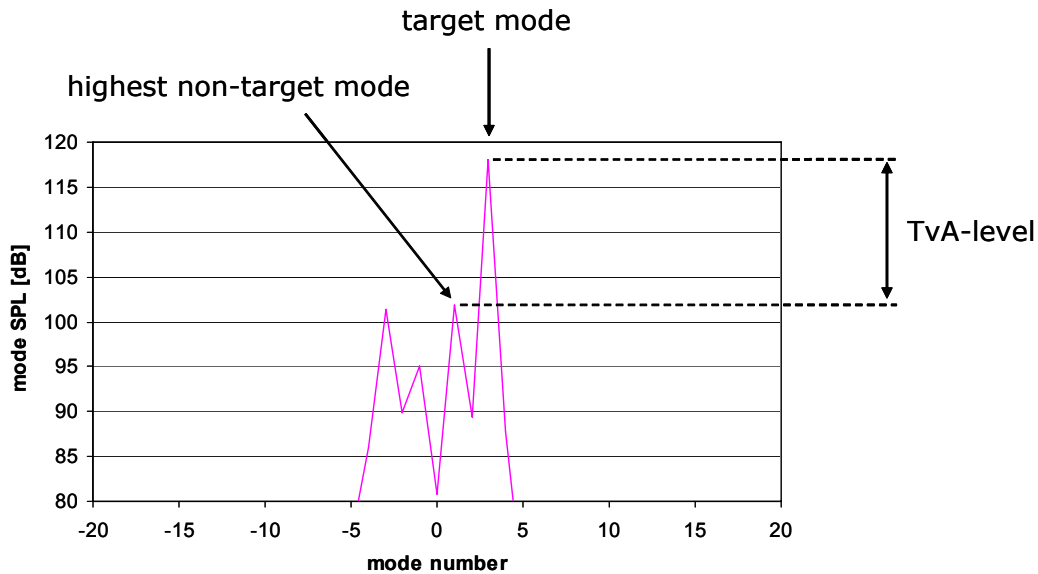


Figure 11. Definition of TvA-level.

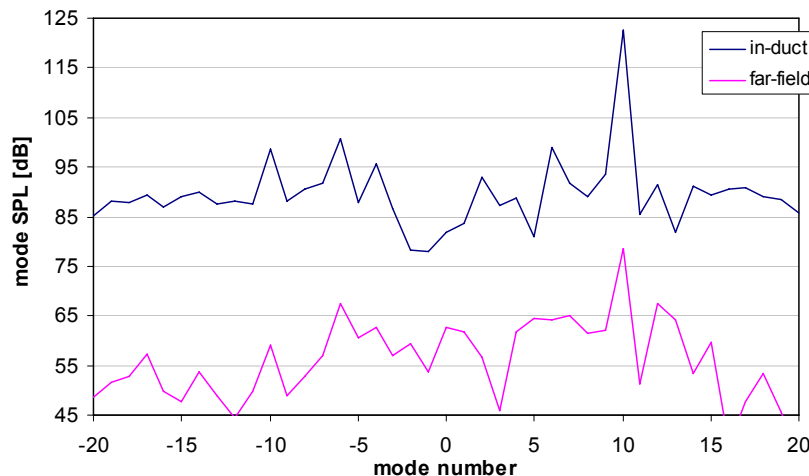


Figure 12. Mode spectra calculated by the PC method,  $M = 0.6$ ,  $f = 5600$  Hz,  $\theta = 105^\circ$ , target  $m = 10$ .

## VI. Conclusion

For the determination of azimuthal modes of tonal sound, there are two suitable techniques: the CC method and the PC method. For in-duct mode measurements, where the (boundary layer) noise is incoherent, the CC method is probably the best choice, because of the very large array gain. In the far-field the CC method may be less suitable, since the noise is no longer incoherent. Also, loss of coherence may have an adverse effect. Then, a good alternative is the PC method, provided that the SP-levels are sufficiently high, say higher than 6 dB.

The mode synthesizer of EADS-IW performed well at the entire range of frequencies that were measured (up to 16800 Hz). TvA-levels were found up to 22.1 dB in the duct and 20.1 dB in the far field. Low TvA-levels at part of the data points can be explained by deviations of the axisymmetry or by far-field directivity.

## Acknowledgments

This study was carried out within the research project TURNEX (TURbomachinery Noise radiation through the Engine eXhaust), which is sponsored by the European Union (6<sup>th</sup> framework). The authors thank Henk van der Wal, Edward Rademaker, Onno Stallinga, Corné Boons, and Marko Beenders for their valuable contributions to the tests. DNW is acknowledged for the use of their data acquisition equipment.

## References

- <sup>1</sup>Sarin, S.L., and Rademaker, E.R., "In-Flight Acoustic Mode Measurements in the Turbofan Engine Inlet of Fokker 100 Aircraft", AIAA-paper 93-4414, October 1993.
- <sup>2</sup>Rademaker, E.R., Sijtsma, P., and Tester, B.J., "Mode Detection with an Optimised Array in a Model Turbofan Engine Intake at Varying Shaft Speeds", AIAA Paper 2001-2181, May 2001.
- <sup>3</sup>Farassat, F., Nark, D. M., and Thomas, R.H., "The Detection of Radiated Modes from Ducted Fan Engines", AIAA Paper 2001-2138, May 2001.
- <sup>4</sup>Amiet, R.K., "Correction of Open Jet Wind Tunnel Measurements for Shear Layer Refraction", AIAA Paper 75-532, March 1975.